PON 20- SPRAY-DRIED POWDER GRANULOMETRY: INFLUENCE ON THE POROUS MICROSTRUCTURE OF POLISHED PORCELAIN TILE

Helton J. Alves, Fábio G. Melchiades and Anselmo O. Boschi*

Laboratório de Revestimentos Cerâmicos (LaRC)
Departamento de Engenharia de Materiais (DEMa)
Universidade Federal de São Carlos (UFSCar)
Rod. Washington Luiz, Km. 235, 13574-970
São Carlos, SP, Brazil
*E-mail: daob@ufscar.br

ABSTRACT: The low porosity of porcelain tile is the result of strict control of the material's processing conditions (milling of raw materials, compaction and sintering) and the characteristics of the raw materials used in its formulation (formation of liquid phases). Sealed pores remaining after the manufacturing process are revealed at the surface after polishing and are the main factor responsible for staining the product. The porous microstructure of the sintered material depends on the characteristics of the porous microstructure of the green compact and on how the densification process evolves during sintering. The present work evaluated how the size distribution of spray-dried granules acts upon the porous microstructure of green compacts and of polished porcelain tile. The results revealed that minor adjustments in the granulometric distribution curve can reduce the visibility of stains on the polished surface, thus improving this property.

Keywords: Stain resistance; Porcelain; Porosity; Microstructure-prefiring; Microstructure-final.

1. INTRODUCTION

Porcelain tile is a ceramic product that stands out for its low water absorption and high mechanical strength. In general, the properties of the product result from its low porosity due to the processing conditions (high degree milling of raw materials, high force compaction and sintering temperature), and the potential of the raw materials to form liquid phases during sintering (high densification). However, in the case of polished porcelain, the sealed pores remaining after the manufacturing process may impair some of its technical properties, such as its stain resistance.[1,2,3,4]

Sealed pores are the result of incomplete densification of the material during sintering, and depend basically on the microstructure of the green compact and on the thermal cycle adopted. With respect to the green compact, the main variables that may interfere in the characteristics of the porous microstructure are particle and grain size distribution, morphology, humidity and pressing pressure.[5,6]

There are basically two types of pores that make up the microstructure of the green compact: intragranular pores (spaces between the particles that comprise the grains) and intergranular pores (set of voids that form during packing of the granules). Another type of pore that can also frequently be found inside larger grains results from the spray-drying process and is referred to by some authors as "hollow".[7,8] This type of "hollow" can be classified as a kind of intergranular pore in view of its similar size and characteristics. Experiments conducted by BELTRÁN [7] indicated that part of the medium-sized or large sealed pores in the microstructure of the end product are probably associated with the use of spray-dried pastes, more specifically with the characteristic "hollow" granules of the agglomerates that constitute these pastes. However, the author's results were not conclusive, so they require careful interpretation. The author studied extreme conditions, evaluating the influence of the use of distinct specific granulometric ranges on the porosity of the final product (very fine granules obtained after grinding in a mortar and pestle, or granules with a very narrow

range of diameters), which are completely unlike the viable industrial conditions for the use of powder for pressing.

The present work, in contrast, seeks to correlate the porous microstructure of the green compact with the closed porosity and stain resistance of the end product. To this end, alterations were made in the green compact microstructure through the preselection of granules of a standard spray-dried paste, originating distinct pastes with varied granule sizes. These alterations were made while the remaining process variables were kept constant, thus allowing for an evaluation solely of the effect of the granule size distribution on the final porous microstructure.

2. MATERIALS AND METHODS

For this study, an industrial spray-dried paste was selected, called STD, which is currently used in the manufacture of polished porcelain tile.

2.1. PRESELECTION AND CHARACTERISTICS OF THE SPRAY-DRIED GRANULES

Initially, part of the spray-dried powder of the STD paste was separated by sieving into three granulometric fractions: < 150μm (FINE), 150-300μm (MEDIUM) and > 300 μm (COARSE). The morphology of the grains comprising these fractions was evaluated in a digital optical microscope (Olympus MIC-D). Four granulometric compositions were then prepared with the spray-dried powder (MM, M, G and F), each containing different percentages of preselected granules, as shown in Table 1. For purposes of comparison, the STD standard sample was also evaluated. In addition, the possibility of heterogeneities in the chemical composition of the spray-dried granules of different sizes was also checked, since that might affect the results of this work, for the presence of microregions with distinct compositions can cause gradients of fusibility and densification during sintering, thereby altering the characteristics of the resulting pores. Thus, the FINE and COARSE granulometric fractions were analyzed chemically by X-ray fluorescence (Philips MagiX Spectrometer).

Table 1 – Granulometric compositions evaluated.

Compositions	Spray-dried powder (mass %)		
	< 150 μm (FINE)	150 - 300 μm (MEDIUM)	> 300 μm (COARSE)
MM	15,0	70,0	15,0
M	30,0	40,0	30,0
G	15,0	30,0	55,0
F	55,0	30,0	15,0
STD	10,0	41,0	49,0

2.2. CHARACTERIZATION OF THE GREEN MICROSTRUCTURE

Several 6.0 x 2.0 cm test specimens of each granulometric composition were prepared under the following conditions: spray-dried powder containing 0.060 kg water/kg of dry paste pressured under a pressure of 400 kgf/cm^2. The test specimens were oven-dried at 110ºC up to constant weight, after which their apparent density was evaluated by the geometric method and their porosity by mercury porosimetry (Micromeritics AutoPore III).

2.3. CHARACTERIZATION OF THE MICROSTRUCTURE AFTER SINTERING

The choice of sintering temperature of the MM, M, G, and F test specimens was based on the previously determined variation of linear shrinkage and water absorption with sintering tempertature of the STD spray-dried paste (Fig. 1), under the conditions described in item 2.2. Because the maximum densification of STD occurs at 1210ºC, this sintering temperature was selected for the other compositions.

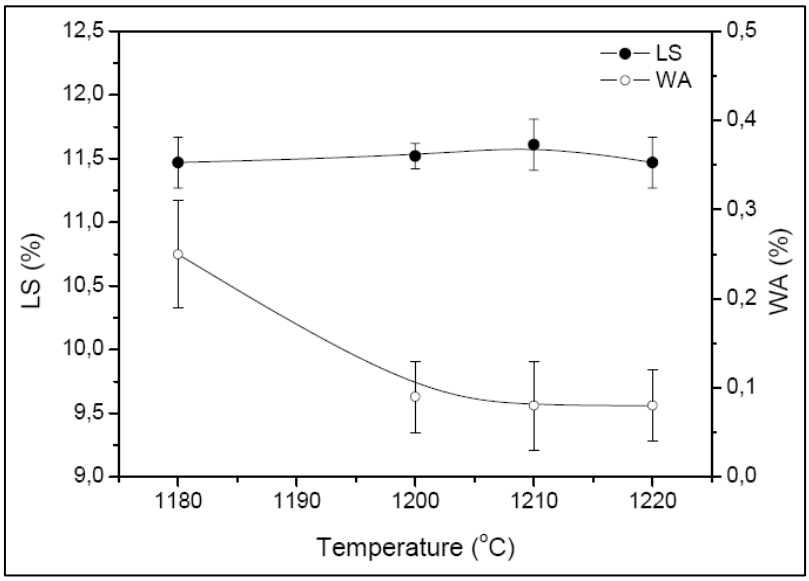

Fig. 1 – Variation of Linear Shrinkage (LS) and Water Absorption (WA) with sintering temperature of the STD spray-dried paste.

The oven-dried test specimens were fired in an electric laboratory furnace using a heating cycle of approximately 55 min and an 8-min threshold at 1210ºC. After sintering, the following values were determined:

- Water absorption (WA) by the water boiling method for two hours, following the ISO 10545-3 standard;[9]
- Apparent porosity (ε_A) by the Archimedes principle;
- Total porosity (ε) and sealed porosity (ε_F), based on equations:

$$\varepsilon = 1 - \left(\frac{\rho_C}{\rho_R} \right) \quad (1)$$

$$\varepsilon_F = \varepsilon - \varepsilon_A \quad (2)$$

where ρ_C is the apparent density and ρ_R corresponds to the absolute density (determined by helium gas pycnometry –x Quantachrome Ultrapycnometer 1000).

The sintered test specimens were then sandpapered and polished with alumina paste in a rotary disc in order to simulate industrial polishing. The characteristics of the samples surface microstructure after polishing were determined from digital images (micrographs) obtained by scanning electron microscopy (SEM, Leo Stereoscan 440). The analysis of the digital images using Image-Pro 4.5 Plus software allowed for the determination of the percentage corresponding to the area covered by pores in relation to the total area of the analyzed images, the distribution of their diameters, and the morphological aspects (aspect ratio).

Concomitantly, the polished test specimens were subjected to the stain test, according to the procedures of the ISO 10545-14 standard.[10] The staining agents used were chrome green (recommended by the standard) and soil (simulating everyday conditions). The intensity of the stains was evaluated by the difference in coloring, ΔE^*, between the surface before staining and after cleaning the area to which the staining agent was applied.[10] The values of ΔE^* were determined by diffuse reflectance spectrophotometry (Konica Minolta CM – 2600d), applying an observation pattern of 10º and standard D65 light (equivalent to daylight), based on the following equation:

$$\Delta E^* = \sqrt{\left(L_0^* - L^* \right)^2 + \left(a_0^* - a^* \right)^2 + \left(b_0^* - b^* \right)^2} \quad (3)$$

where L_0^* a_0^* b_0^* and L^* a^* b^* are the chromatic coordinates of the specimens before staining and after the cleaning procedures, respectively. The higher the value of ΔE^* the stronger the stain observed on the surface.

Based on the results of the experiments, an evaluation was made of the real influence of the granulometric distribution of the spray-dried powder on the porous microstructure after sintering and, hence, on the stain resistance.

3. RESULTS AND DISCUSSION

3.1. CHARACTERISTICS OF THE SPRAY-DRIED POWDER

Table 2 shows the results of the chemical analysis of the preselected FINE and COARSE granules. Note that the chemical compositions are very similar, without appreciable differences, thus eliminating the possibility of interference of this variable on the results of this work.

Table 2 – Chemical analysis of the STD spray-dried powder.

Oxides (%)	STD	
	FINE	COARSE
P.F.	3,37	3,43
SiO_2	56,91	57,16
Al_2O_3	24,42	24,65
Fe_2O_3	0,28	0,28
TiO_2	0,10	0,09
CaO	1,07	1,08
MgO	0,43	0,42
K_2O	0,96	0,96
Na_2O	2,42	2,49
Li_2O	0,54	0,54
ZrO_2	10,16	9,75
P_2O_5	0,15	0,15

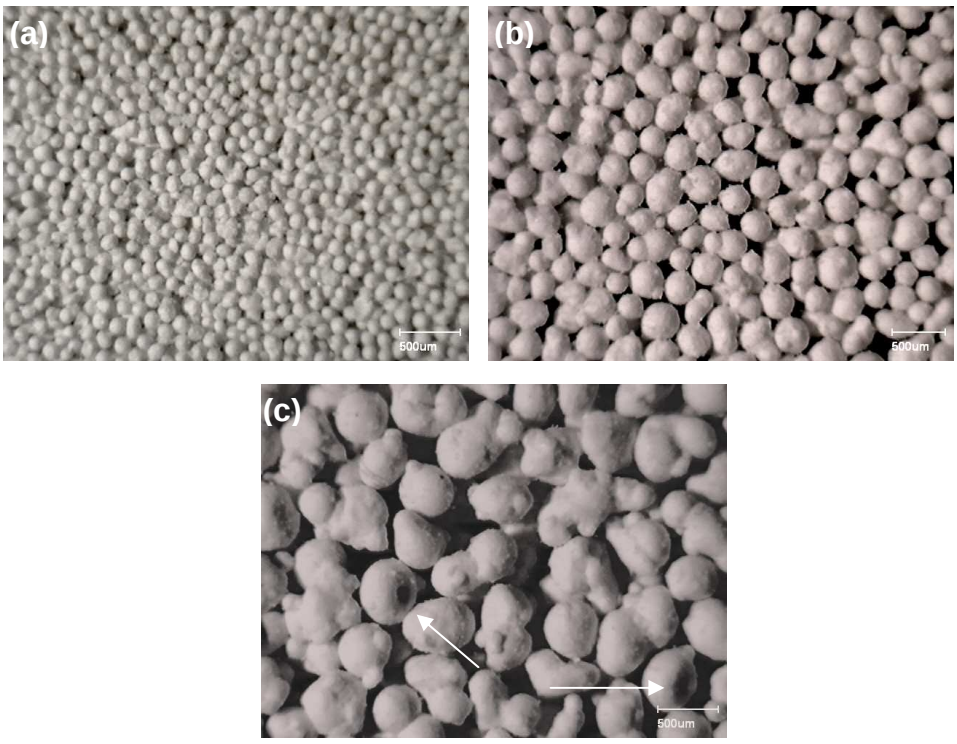

Fig. 2 – MOD micrographs of distinct granulometric fractions of the STD spray-dried powder: (a) < 150 μm, (b) 150 - 300 μm, and (c) > 300 μm.

Figure 2 indicates that the morphology of the granules varies according to their size. The smaller the granule the greater the tendency for a spherical shape and the larger the surface area. Thus, the FINE granules, Fig. 2(a), have a regular morphology with a greater

tendency to be spherical, while the COARSE grains, Fig. 2 (c), show an irregular morphology and a smaller specific surface area.

3.2. GREEN MICROSTRUCTURE

After pressing, the values of apparent density, ρ_C, obtained for the test specimens revealed that the granulometric compositions evaluated showed very similar degrees of compaction (Table 3), indicating that the total volume of pores generated in the green compact is the same, independently of the initial granule size distribution. This was confirmed by the results of the porosimetry analysis (Fig. 3), which shows that the volume of Hg penetrated into the test specimens of all the granulometric compositions tested here was practically the same.

Although the pore volume is constant and the distribution of Hg penetration diameters is similar (Fig. 3), it is important to point out that there are some differences between the green compacts analyzed. As can be seen, only M, G and STD have pores with penetration diameters of 1,0 to 4,0 μm, which may be associated with the higher percentage of COARSE granules used in these compositions (Table 1).

Table 3 – Apparent density of the green test specimens.

Green test specimens	ρ_C (g/cm^3)
MM	1,85 ± 0,01
M	1,85 ± 0,02
G	1,86 ± 0,01
F	1,84 ± 0,01
STD	1,83 ± 0,01

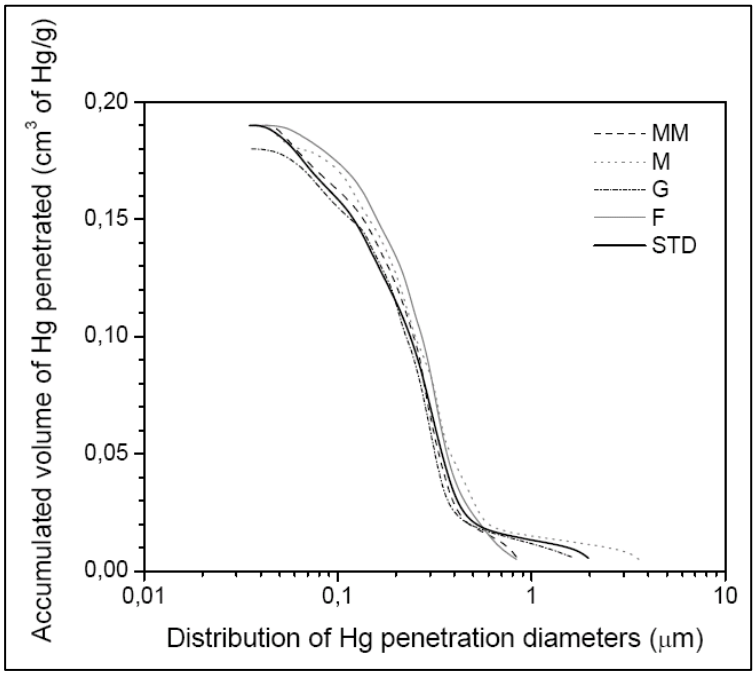

Fig. 3 – Distribution of the mercury penetration diameters (green compact).

3.3. FINAL MICROSTRUCTURE

Table 4 presents the results of the characterization of the test specimens' porosity after sintering. Note that the values of WA, ε_A, ε_F and ε obtained for all the evaluated compositions are very similar, suggesting that the pores have the same volumetric fraction. However, it should be pointed out that MM, M, G and F have a slightly higher total pore volume than that of the STD standard.

Table 4 – Characterization of the porosity of the sintered test specimens.

Granulometric compositions	WA (%)	ε_A (%)	ε_F (%)	ε * (%)
MM	0,10 ± 0,05	0,26 ± 0,11	8,06 ± 0,20	8,32 ± 0,16
M	0,12 ± 0,03	0,31 ± 0,08	8,13 ± 0,11	8,44 ± 0,17
G	0,10 ± 0,05	0,25 ± 0,12	8,18 ± 0,17	8,42 ± 0,18
F	0,08 ± 0,02	0,20 ± 0,04	8,32 ± 0,18	8,52 ± 0,16
STD	0,06 ± 0,01	0,15 ± 0,01	7,59 ± 0,01	7,74 ± 0,01

* The value of ρ_R obtained for the calculation of ε was 2,740 g/cm^3.

Under the conditions found here, in which the microstructures of the green compacts are similar (pore volume) and porosity after sintering is constant (total pore volume, apparent porosity and sealed pores), the only possible effect caused by the use of different granulometric distributions, according to the methodology adopted here, would be related to the size and morphology of the pores in the final microstructure. About this point, it is worth emphasizing that two samples can present the same pore volume but distinct size distributions, which may suffice to modify their surface properties, such as stain resistance. To verify the validity of this hypothesis, the fired test specimens were polished and then analyzed by SEM and evaluated with respect to their stain resistance.

3.3.1. STAIN RESISTANCE

Table 5 lists the results of the stain resistance test, indicating similar behaviors for the evaluated compositions (MM, M, G and F) and STD. Stains are still visible even after the most aggressive cleaning process with chloric acid (3% v/v), and were classified as unremovable, belonging to Class 1 cleanability. The only difference found was in regard to the green chrome staining agent applied to the test specimens of the MM composition, which was removed by cleaning with abrasive alkaline paste, and was classified as 3 (the higher the cleanability class the easier the removal of the stain and the less aggressive the cleaning process whereby the stain can be removed).

Although a large part of the test specimens presented unremovable stains after the cleaning procedures, the intensity of the stains showed visible differences, with the MM and F compositions showing stains of lesser and greater intensity, respectively (Fig. 4). The use of a diffuse reflectance spectrophotometer to evaluate the intensity of stains or the degree of cleanability of the product, a quantitative evaluation, was considered very promising since, besides standardizing the evaluation of the surface after the stain tests, it eliminates possible deviations caused by the qualitative visual analysis recommended by the ISO 10545-14 standard.[10]

Table 5 – Results of the stain resistance test of the polished test specimens.

Staining agent	MM	M	G	F	STD
Green chrome	3	1	1	1	1
Soil	1	1	1	1	1

3.3.2. IMAGE ANALYSIS

Eight micrographs were recorded at random points of the surface of each polished test specimen (Fig. 5), which were then treated and analyzed using Image-Pro 4.5 Plus software. The results of the image analysis (pore areas, mean diameter and aspect ratio) are presented in Table 6 and in Figures 6 and 7, respectively.

Table 6 – Area corresponding to the pores.

Mean pore coverage area / total area of the image (%)				
MM	**M**	**G**	**F**	**STD**
5,03 ± 0,58	6,60 ± 0,83	7,28 ± 0,72	8,57 ± 0,66	6,71 ± 0,56

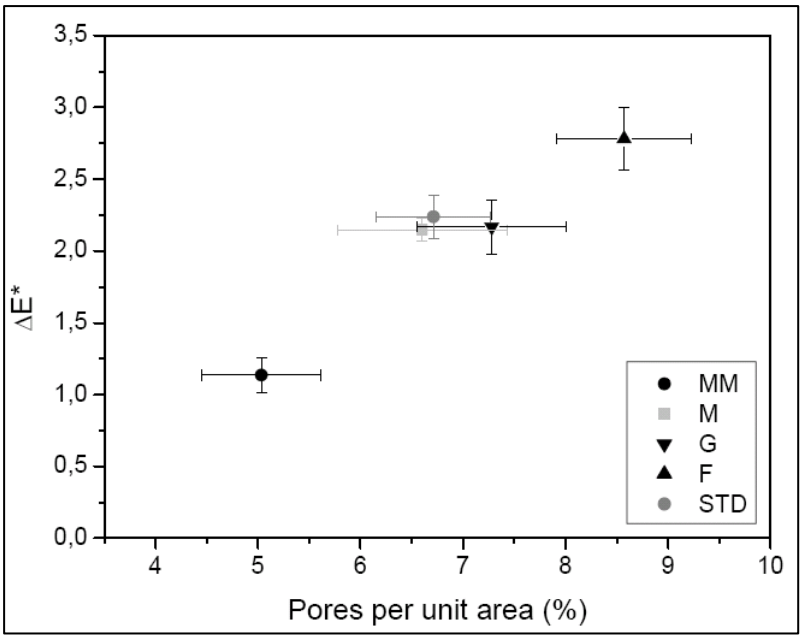

Fig. 4 – Variation of cleanability according to the surface pore area of polished test specimens.

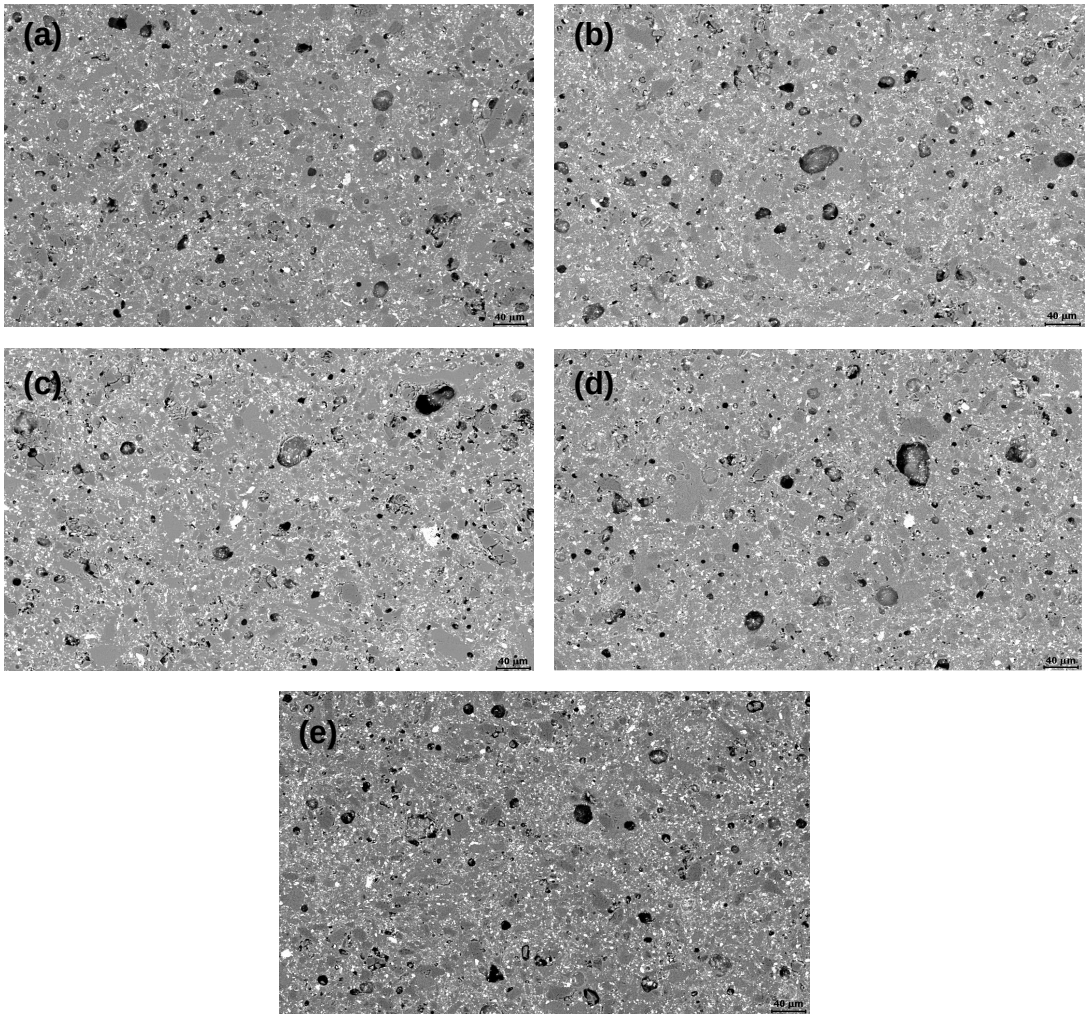

Fig. 5 – SEM micrographs of the surface of the polished test specimens: (a) MM, (b) M, (c) G, (d) F, and (e) STD.

The image analysis revealed that the pore size distribution (Fig. 6) and the aspect ratio (Fig. 7) of the test specimens of MM, M, G, F and STD were very similar, confirming their similar behavior in the staining test. However, the following points deserve to be mentioned:

- All the compositions have very similar percentages of pores with diameters ranging from 5 to 20 μm (critical for staining), which justifies their similar stain resistance behavior;[11]
- In general, the pores of F have a more irregular shape than those of the other compositions, which may be due to the type of pore formed when a high percentage of FINE granules are used.

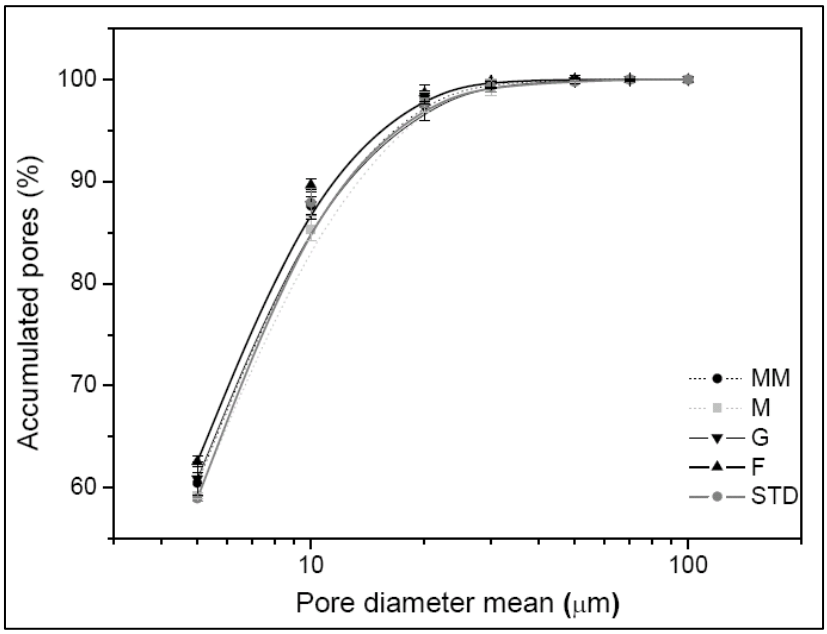

Fig. 6 – Distribution of surface pore diameters.

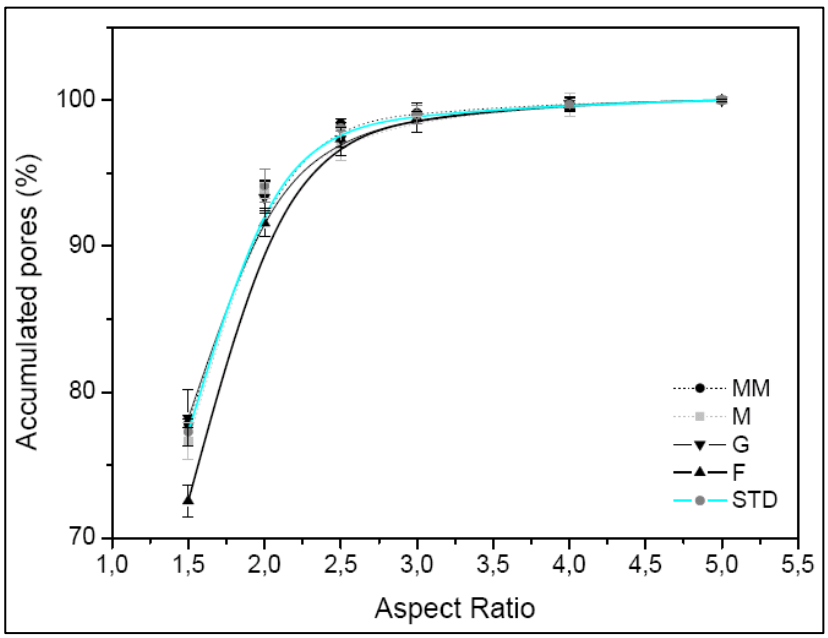

Fig. 7 – Distribution of surface pore aspect ratio.

In this case, where the pore size distribution is similar, the area of pore coverage seems to contribute to the intensity of the visible stain. As Table 6 indicates, the areas corresponding to the pores of MM (weaker stain) and F (stronger stain) are the smallest and the largest, respectively, among all the analyzed samples. Fig. 4 confirms this behavior. Note

that the values of ΔE^* increase as the area of pores increases, i.e., the stain is stronger where the area of pores is the largest.

It should be noted that the analysis of the digital images reveals the pore coverage area in relation to the area of the image, and not the volume occupied by the pores. In some cases where the pores present a regular spherical morphology distributed uniformly throughout the material, the pore area may be related with the volume to a certain degree. In the case under study, this relation is not possible since the pore morphology is irregular, and the depths of the pores cannot be determined by this type of two-dimensional analysis. Therefore, comparing the compositions evaluated here, the differences in pore areas may be attributed to a possible pore orientation, since the volume was very similar (Table 4). In the case of the compositions with larger pore areas (F), the pore depth should be shallower. On the other hand, the compositions with smaller pore areas (MM) should be constituted of deeper pores. The remaining compositions (M, G and STD) have intermediary characteristics between the two aforementioned situations.

3.4. RELATIONSHIP BETWEEN THE GRANULOMETRY OF THE SPRAY-DRIED POWDER AND THE POROUS MICROSTRUCTURE AFTER SINTERING

Several aspects should be taken into consideration for a better understanding of the results of this work:[12]

a) Composition with high FINE (F) content: in this case, the initial arrangement of the FINE granules favors the formation of a large quantity of intergranular pores after pressing. FINE granules are generally denser and have a low plastic deformation capacity, which limits the reduction of the volume of pores in the green compact, however efficient the pressing stage may be. After sintering, the microstructure is composed of a high number of pores, the sum of whose areas justifies the larger area of coverage in relation to the area of the image (stronger stain).

b) Composition with high MEDIUM (MM) content: the good deformability of the MEDIUM granules gives the powder a better initial packing condition. Although the volume of pores of the green compact was not inferior to that of the other compositions, the deformation capacity of the granules contributed to reduce the number of pores, possibly oriented (greater depth) so that the area corresponding to the surface pores after sintering was less visible (weaker stain).

c) Compositions with high COARSE contents (G and STD): COARSE granules generate large pore volumes in powder ready for pressing. Although COARSE granules deform easily (lower density), their irregular morphology prevents the reduction of pore volume. Therefore, green compact shows intergranular pores with large diameters, composed basically of residual pores and "hollow" granules. The final porous microstructure has intermediary characteristics between (b) and (c).

Composition M presents properties between (a) and (b).

4. CONCLUSIONS

The results of this study led to the following conclusions:

- The granulometric distribution of the spray-dried paste STD in the conditions evaluated in this work does not interfere significantly in the pore size distribution of the material after sintering. Distinct granulometric compositions led to the same porosity profile in the sintered product.
- The only effect cause by the use of granules with distinct characteristics was on the area of surface pores, which was quantified by image analysis. In this case, the area occupied by surface pores is directly related to the intensity of the stains, i.e., the larger the area the more visible the stain.
- The use of the diffuse reflectance spectrophotometer proved efficient in the evaluation of staining since, besides quantifying the intensity of the stains, it reduced the errors resulting from the visual analysis recommended by the ISO 10545-14 standard.[10] The values of ΔE* obtained showed a good correlation with the porosity.

- Although some authors suggest that "hollow" granules are responsible for the formation of porous microstructures that are more susceptible to staining, no evidence was found in this study to confirm this hypothesis.

REFERENCES

1. Rastelli, E., Tucci, A., Esposito, L. and Selli, S., Stain resistance of porcelain stoneware tile: mechanisms of penetration of staining agents and quantitative evaluation. *Ceram. Acta*, 2002, **14**(1), 30–37.
2. Sánchez, E., Technical considerations on porcelain tile products and their manufacturing process. Part II. *Interceramic*, 2003, **52**(3), 132–139.
3. Sánchez, E., Porcelain tile microstructure: implications for polished tile properties. *J. Eur. Ceram. Soc.*, 2006, **26**, 2533-2540.
4. Dondi, M., Raimondo, M. and Zanelli, C., Stain resistance of ceramic tiles. *Ceramic World Review*, 2008, **77**, 82-91.
5. Amorós, J. L., Fuentes, A. B., Navarro, J. E. E., Medall, F. N., Caracteristicas de polvos ceramicos para prensado. *Bol. Soc. Esp. Ceram. Vidr.*, 1987, **26**, 31-37.
6. Amorós, J. L., Orts, M. J., García-Ten, J., Gozalbo, A. and Sánchez, E., Effect of the green porous texture on porcelain tile properties. *J. Eur. Ceram. Soc.*, 2007, **27**, 2295-2301.
7. Beltrán, V., Ferrer, C., Bagán, V., Sánchez, E., Garcia, J. and Mestre, S., Influence of pressing powder characteristics and sintering temperature on the porous microstructure and stain resistance of porcelain tile. In *Proceedings of the IV World Congress on Ceramic Tile Quality. Cámara Oficial de Comercio y Navegación*, 1996, 133-148.
8. Amorós, J. L., Cantavella, V., Jarque, J. C., Felíu, C., Fracture properties of spray-dried powder compacts: effect of granule size. *J. Eur. Ceram. Soc.*, 2008, **28**, 2823-2834.
9. International Standard ISO 10545-3, Ceramic Tile – Part 3: Determination of water absorption, apparent porosity, apparent relative density and bulk density, 1997.
10. International Standard ISO 10545-14, Ceramic Tiles – Part 14: Determination of resistance to stains, 1997.
11. Alves, H. J., Minussi, F. B., Melchiades, F. G., Boschi, A. O., Porosidade susceptível ao manchamento em porcelanato polido. *Cerâmica Industrial*, São Paulo, Brasil, 2009, **14** (1), 21-26.
12. Arantes, F. J. S., Galesi, D. F., Quinteiro, E., Boschi, A. O., O manchamento e a porosidade fechada de grês porcelanato. *Cerâmica Industrial*, São Paulo, Brasil, 2001, **6**(3), 18-25.